Chapter 3

A Noncoherent Pseudo-Noise Acquisition Scheme for Direct-Sequence Spread-Spectrum Systems Using an Auxiliary Signal

3.1 Introduction

As mentioned in Chapter 2, a new acquisition scheme was proposed in [26], which was able to reduce acquisition time. Coherent demodulator was assumed. The scheme consists of two parts, phase alignment detector and VCC loop, as shown in Figure 2.6. An auxiliary signal in VCC loop is used for correlation with the incoming signal. The auxiliary signal is a linear combination of the PN signal and its shifted versions. By design, the cross-correlation of the auxiliary and the PN signal has a triangle shape with a period equal the period of the PN signal. Such a cross-correlation function enables the receiver to identify the direction of phase update toward the synchronized phase.

In this chapter, the idea of using an auxiliary signal is extended to noncoherent acquisition. Section 3.2 describes the proposed scheme. Section 3.3 evaluates the probabilities of detection and false alarm. Finally, Section 3.4 presents some simulation results.

3.2 The Proposed Noncoherent Scheme

For the DS/SS systems the input signal without data modulation is given in [3] as

$$s(t) = \sqrt{2P}c(t-\tau)\cos(\omega_c t - \theta) + n(t), \tag{3.1}$$

where $c(t)$ is the PN signal, ω_c and θ are the carrier frequency and phase, P is the average power of the received signal, τ is the phase of the PN signal due to propagation delay, and $n(t)$ is a zero-mean white Gaussian noise with power spectrum density (PSD) of $N_0/2$. For convenience, we use the equivalent baseband signal of $s(t)$, which is

$$u(t) = \sqrt{2P}c(t-\tau)e^{-j\theta} + z(t). \tag{3.2}$$

The carrier phase θ is assumed to be a uniform random variable, and $z(t)$ is a zero mean white Gaussian process with PSD of $2N_0$. It can be written as

$$z(t) = z_R(t) + jz_I(t), \tag{3.3}$$

where $z_R(t)$ and $z_I(t)$ are the real part and imaginary part of $z(t)$, respectively.

Let $\hat{\tau}$ be the phase of the local PN signal and auxiliary signal. The phase difference is defined by

$$e_\tau = \hat{\tau} - \tau . \tag{3.4}$$

The function of an acquisition scheme is to obtain the phase estimate $\hat{\tau}$ such that the error e_τ is within some specified range such as $\pm \frac{T_c}{2}$, where T_c is the chip duration.

The proposed noncoherent acquisition system is depicted in Figure 3.1. It consists of two parts: voltage controlled clock (VCC) loop and phase alignment detector. The VCC loop uses advanced and delayed versions of an auxiliary signal for correlating with the incoming signal. The auxiliary signal $\alpha(t)$ is designed so that its cross-correlation with the PN signal will indicate the direction for updating the phase of the auxiliary signal. The phase alignment detector decides whether the phase supplied by the VCC loop is within some specified range of the phase of the incoming PN signal. Note that phase alignment detection uses a local PN signal to correlate with the incoming PN signal. In the following subsections we describe the auxiliary signal, the VCC loop, and the alignment detector.

3.2.1 Auxiliary Signal $\alpha(t)$

The auxiliary signal $\alpha(t)$ is defined in [26] by

$$\alpha(t) = \sum_{i=-\frac{N-3}{2}}^{\frac{N-3}{2}} \left[\frac{N-1}{2} - |i| \right] c(t - iT_c), \tag{3.5}$$

where N is the period of the PN sequence $\{c_k\}$, i.e. $c_{k+N} = c_k$, and $c(t)$ is the PN signal given by

$$c(t) = \sum_{k=-\infty}^{\infty} c_k P_{T_c}(t - kT_c), \tag{3.6}$$

where $c_k = \pm 1$ is the k^{th} chip of the PN sequence. Note that $c(t)$ has period of NT_c. P_{T_c} is the unit-amplitude rectangular pulse shape in the interval $[0, T_c]$.

The cross-correlation of $c(t)$ and $\alpha(t)$ is

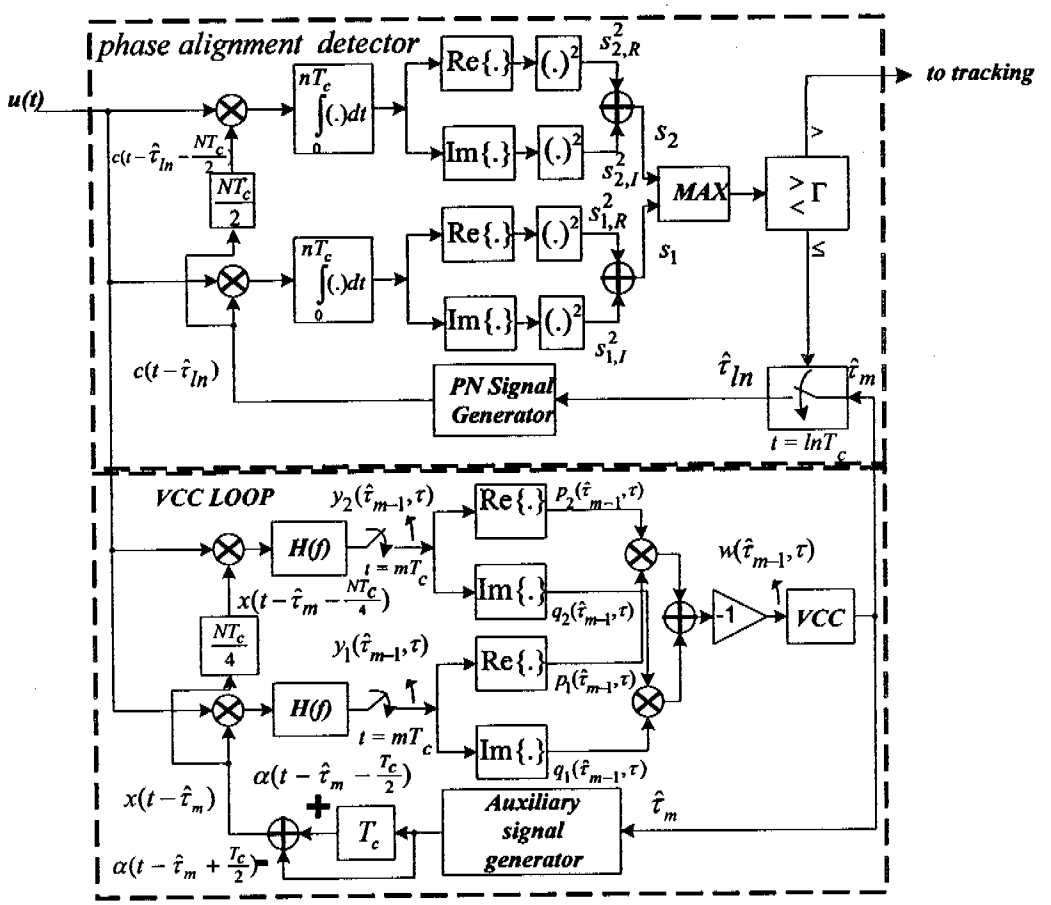

Figure 3.1: The proposed noncoherent PN acquisition scheme

$$R_{c\alpha}(\beta)=\frac{1}{NT_c}\int_0^{NT_c}c(t+\beta)\alpha(t)dt$$

$$=\begin{cases}\dfrac{(N-1)(N+3)}{4N}-\dfrac{N+1}{NT_c}|\beta|, & |\beta|\le\dfrac{(N-1)T_c}{2}\\[2ex] -\dfrac{(N-1)^2}{4N}, & \dfrac{(N-1)T_c}{2}<\beta<\dfrac{(N+1)T_c}{2}.\end{cases}\qquad(3.7)$$

This is plotted in Figure 3.2. Note that it is periodic with period NT_c, which is the same as the period of $c(t)$.

In the VCC loop, we generate a signal $x(t)$ which is the difference between delayed and advanced versions of $\alpha(t)$. Specifically, we let

$$x(t) = \alpha\left(t - \frac{T_c}{2}\right) - \alpha\left(t + \frac{T_c}{2}\right). \tag{3.8}$$

The cross-correlation of $x(t)$ with $c(t)$ is

$$\begin{aligned} R_{cx}(\beta) &= \frac{1}{NT_c}\int_0^{NT_c} c(t+\beta)x(t)dt \\ &= R_{c\alpha}\left(\beta + \frac{T_c}{2}\right) - R_{c\alpha}\left(\beta - \frac{T_c}{2}\right), \end{aligned} \tag{3.9}$$

which is shown in Figure 3.3. It is periodic with period NT_c.

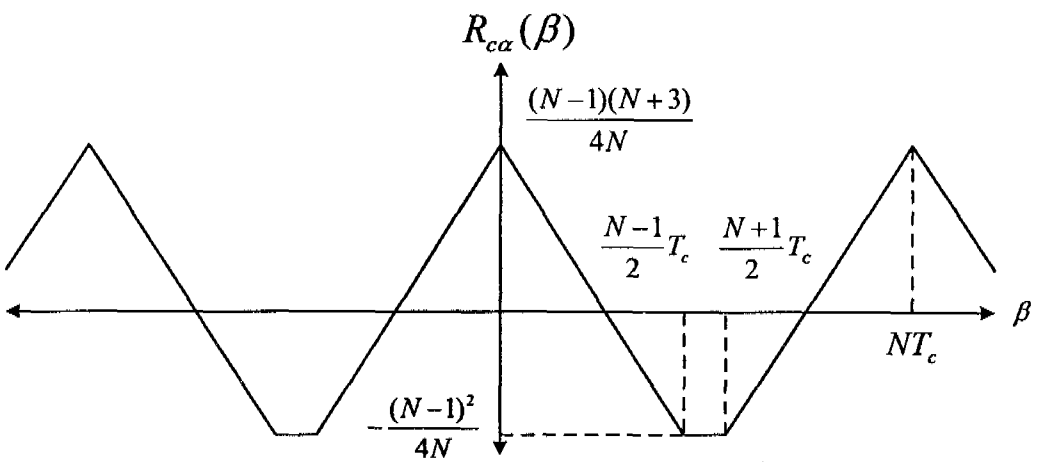

Figure 3.2: The periodic cross-correlation $R_{c\alpha}(\beta)$

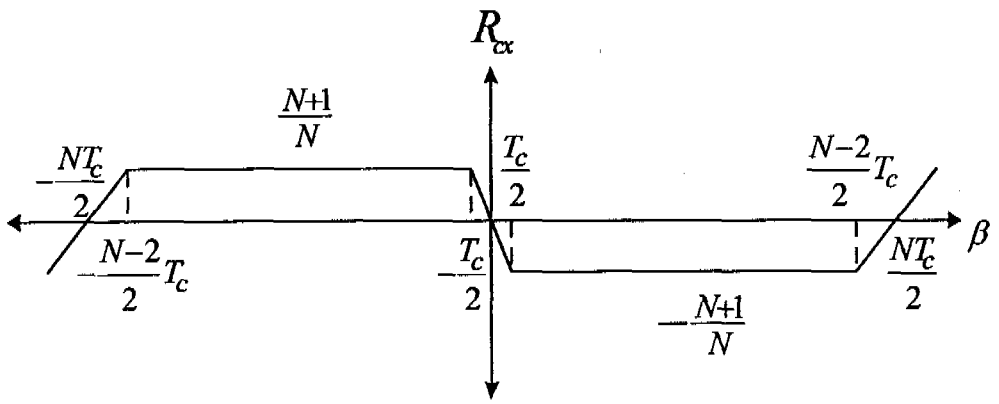

Figure 3.3: The periodic cross-correlation $R_{cx}(\beta)$

3.2.2 VCC Loop

The VCC loop is the lower part of Figure 3.1. The function of this part is to update the phase of the local PN signal by updating the phase of the auxiliary signal. The received signal $u(t)$ is correlated with $x(t-\hat{\tau}_m)$ and $x(t-\hat{\tau}_m-\frac{NT_c}{2})$. The results of correlation are filtered by $H(f)$ and then sampled at $t = mT_c$, where $m = \{0, 1, 2, \ldots\}$. For noncoherent acquisition, the carrier phase θ is unknown. Note that noncoherent acquisition is more realistic than coherent acquisition, since θ is normally not available during acquisition. To eliminate the unknown carrier phase, we form two products: one as the product of the real parts of the two signals after the filters, and the other is the product of the imaginary parts. The two products are summed and inverted to obtain $w(\hat{\tau}_{m-1}, \tau)$.

The VCC computes an estimated $\hat{\tau}_m$ of the phase by updating the previous estimate $\hat{\tau}_{m-1}$ using $w(\hat{\tau}_{m-1}, \tau)$. Specifically, the updated estimate is

$$\hat{\tau}_m = \hat{\tau}_{m-1} + K_{VCC} w(\hat{\tau}_{m-1}, \tau) \tag{3.10}$$

where K_{VCC} is a constant, which must be properly chosen. The value K_{VCC} will be determined at the end of this subsection.

Next, we obtain expressions for signals at various points in the VCC loop. The two filters $H(f)$ are chosen to have an impulse response

$$h(t) = \begin{cases} \frac{1}{M}, & 0 \le t \le MT_c \\ 0, & \text{otherwise} \end{cases}. \tag{3.11}$$

Therefore, it is a moving average filter. The filtered signals can be obtained as

$$y_1(\hat{\tau}_{m-1},\tau)=\frac{\sqrt{2PT_c}}{M}\sum_{k=m-M}^{m-1}\left[v_{k+1}(\hat{\tau}_k,\tau)e^{-j\theta}+\eta_{1,k+1}\right] \tag{3.12}$$

and

$$y_2(\hat{\tau}_{m-1},\tau)=\frac{\sqrt{2PT_c}}{M}\sum_{k=m-M}^{m-1}\left[v_{k+1}\left(\hat{\tau}_k+\tfrac{NT_c}{4},\tau\right)e^{-j\theta}+\eta_{2,k+1}\right] \tag{3.13}$$

where $v_{k+1}(\cdot,\cdot)$ is a signal component, while $\eta_{1,k+1}$ and $\eta_{2,k+1}$ are noise components given by

$$v_{k+1}(\hat{\tau}_k,\tau)=\frac{1}{T_c}\int_{kT_c}^{(k+1)T_c}c(t-\tau)x(t-\hat{\tau}_k)dt \tag{3.14}$$

$$\eta_{1,k+1}=\frac{1}{\sqrt{2PT_c}}\int_{kT_c}^{(k+1)T_c}z(t)x(t-\hat{\tau}_k)dt \tag{3.15}$$

$$\eta_{2,k+1}=\frac{1}{\sqrt{2PT_c}}\int_{kT_c}^{(k+1)T_c}z(t)x(t-\hat{\tau}_k-\tfrac{NT_c}{4})dt\,. \tag{3.16}$$

The real parts of $y_1(\hat{\tau}_{m-1},\tau)$ and $y_2(\hat{\tau}_{m-1},\tau)$ are

$$p_1(\hat{\tau}_{m-1},\tau)=\frac{\sqrt{2PT_c}}{M}\cos\theta\sum_{k=m-M}^{m-1}v_{k+1}(\hat{\tau}_k,\tau)+\frac{\sqrt{2PT_c}}{M}\sum_{k=m-M}^{m-1}\eta_{R1,k+1} \tag{3.17}$$

$$p_2(\hat{\tau}_{m-1},\tau)=\frac{\sqrt{2PT_c}}{M}\cos\theta\sum_{k=m-M}^{m-1}v_{k+1}\left(\hat{\tau}_k+\tfrac{NT_c}{4},\tau\right)+\frac{\sqrt{2PT_c}}{M}\sum_{k=m-M}^{m-1}\eta_{R2,k+1} \tag{3.18}$$

and the imaginary parts are

$$q_1(\hat{\tau}_{m-1},\tau)=\frac{\sqrt{2PT_c}}{M}\sin\theta\sum_{k=m-M}^{m-1}v_{k+1}(\hat{\tau}_k,\tau)+\frac{\sqrt{2PT_c}}{M}\sum_{k=m-M}^{m-1}\eta_{I1,k+1} \tag{3.19}$$

$$q_2(\hat{\tau}_{m-1},\tau)=\frac{\sqrt{2PT_c}}{M}\sin\theta\sum_{k=m-M}^{m-1}v_{k+1}\left(\hat{\tau}_k+\tfrac{NT_c}{4},\tau\right)+\frac{\sqrt{2PT_c}}{M}\sum_{k=m-M}^{m-1}\eta_{I2,k+1} \tag{3.20}$$

where $\eta_{R1,k+1}$, $\eta_{R2,k+1}$, $\eta_{I1,k+1}$, and $\eta_{I2,k+1}$ are real and imaginary parts of (3.15) and (3.16). These are zero-mean Gaussian random variables.

Let us write

$$\hat{\tau}_k - \tau_k = (j_k + \gamma_k)T_c \tag{3.21}$$

$$\hat{\tau}_k + \tfrac{NT_c}{4} - \tau_k = (j'_k + \gamma'_k)T_c, \tag{3.22}$$

where j_k and j'_k are integers and $\gamma_k, \gamma'_k \in (-0.5, 0.5]$. By using the same method in [26], we can express (3.14) to be

$$v_{k+1}(\hat{\tau},0) = c_k\{(0.5+\gamma_k)(\alpha_{k-1-j_k} - \alpha_{k-j_k}) + (0.5-\gamma_k)(\alpha_{k-j_k} - \alpha_{k+1-j_k}) \tag{3.23}$$

and the variance of the four noise terms as

$$\sigma^2_{R1,k+1} = \sigma^2_{I1,k+1} = \frac{1}{SNR}\{(0.5+\gamma_k)(\alpha_{k-1-j_k} - \alpha_{k-j_k})^2 + (0.5-\gamma_k)(\alpha_{k-j_k} - \alpha_{k+1-j_k})^2 \tag{3.24}$$

$$\sigma^2_{R2,k+1} = \sigma^2_{I2,k+1} = \frac{1}{SNR}\{(0.5+\gamma'_k)(\alpha_{k-1-j'_k} - \alpha_{k-j'_k})^2 + (0.5-\gamma'_k)(\alpha_{k-j'_k} - \alpha_{k+1-j'_k})^2, \tag{3.25}$$

where α_k is the k^{th} chip of the auxiliary sequence and SNR is the signal energy per chip to noise PSD ratio, given by

$$SNR = \frac{2PT_c}{N_0}. \tag{3.26}$$

To cancel the effect of θ which is assumed to be a uniform random variable, we form the sum of the products to obtain

$$w(\hat{\tau}_{m-1}, \tau) = -[p_1(\hat{\tau}_{m-1}, \tau)p_2(\hat{\tau}_{m-1}, \tau) + q_1(\hat{\tau}_{m-1}, \tau)q_2(\hat{\tau}_{m-1}, \tau)] \tag{3.27}$$

which consists of a signal term and noise terms. Its expected value can be shown to be

$$\begin{aligned}\overline{w} &= E[w(\hat{\tau}_{m-1}, \tau)] \\ &= -2PT_c^2\left\{\left[R_{c\alpha}\left(e_\tau + \frac{T_c}{2}\right) - R_{c\alpha}\left(e_\tau - \frac{T_c}{2}\right)\right]\left[R_{c\alpha}\left(e_\tau + \frac{(N+2)T_c}{4}\right)\right.\right. \\ &\quad \left.\left. - R_{c\alpha}\left(e_\tau + \frac{(N-2)T_c}{4}\right)\right] + \zeta_I + \zeta_R\right\}\end{aligned} \tag{3.28}$$

where

$$\zeta_R = E\left\{\left(\frac{1}{M}\sum_{k=m-M}^{m-1}\eta_{R1,k+1}\right)\left(\frac{1}{M}\sum_{k=m-M}^{m-1}\eta_{R2,k+1}\right)\right\} = \frac{N+1}{NM(SNR)} \approx \frac{1}{M(SNR)} \tag{3.29}$$

and

$$\zeta_I = E\left\{\left(\frac{1}{M}\sum_{k=m-M}^{m-1}\eta_{I1,k+1}\right)\left(\frac{1}{M}\sum_{k=m-M}^{m-1}\eta_{I2,k+1}\right)\right\} = \frac{N+1}{NM(SNR)} \approx \frac{1}{M(SNR)}. \tag{3.30}$$

Evaluations of ζ_R and ζ_I are present in Appendix A. Since M is a large value, we have $\zeta_R, \zeta_I = 0$, yielding

$$\overline{w} = -2PT_c^2\left[R_{c\alpha}\left(e_\tau + \frac{T_c}{2}\right) - R_{c\alpha}\left(e_\tau - \frac{T_c}{2}\right)\right]\left[R_{c\alpha}\left(e_\tau + \frac{(N+2)T_c}{4}\right) - R_{c\alpha}\left(e_\tau + \frac{(N-2)T_c}{4}\right)\right]. \tag{3.31}$$

Note that (3.31) is a product of (3.9) and its delayed version. It is the delay discriminator characteristic of the VCC loop and plotted in Figure 3.4, which shows a period of NT_c. We see that there are 2 stable points, at $e_\tau = 0$ and $e_\tau = NT_c/2$. If e_τ is initially in the range of $[-NT_c/4, NT_c/4]$, e_τ will converge to zero. Otherwise e_τ will converge to $NT_c/2$. Therefore, the pull-in range is $\pm NT_c/4$.

The determine a choice for the constant K_{VCC}, note that each update at the phase alignment detector should not be lager than T_c to avoid jumping over the correct phase, i.e. $\left|\hat{\tau}_{ln} - \hat{\tau}_{(l-1)n}\right| \le T_c$. Therefore, from (3.10) we set the maximum of $nK_{VCC}|\overline{w}| \le T_c$ which yields

$$K_{VCC} \le \frac{T_c}{n\max|\overline{w}|} \le \frac{N^2}{2nP(N+1)^2 T_c}. \tag{3.32}$$

If K_{VCC} is small, the update step size is small, which means that the acquisition will be longer. Hence, we use the upper limit in (3.32) for the value K_{VCC}.

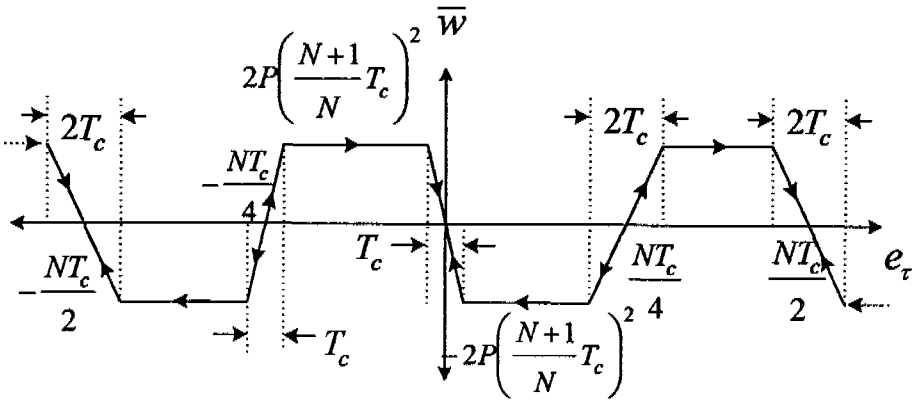

Figure 3.4: VCC Loop discriminator characteristic

3.2.3 Phase Alignment Detector

In Figure 3.1 the upper part is the alignment detector. The received signal is correlated with two waveforms of the local PN signal. The first has a phase determined by the VCC loop. The phase of the other one is delayed by $NT_c/2$. This is because we need to distinguish the two stable points in Figure 3.4. The integration length of each correlator is nT_c seconds. The alignment test is performed at $t = lnT_c$, $l = 1, 2, \ldots$. The magnitude squares of the outputs of the two correlators are compared and the larger one is tested against a threshold. If the threshold is exceeded, the tracking circuit is initiated. Otherwise, the next estimate of $\hat{\tau}$ from the VCC loop is used for the next alignment test. The value n and the threshold Γ need to be designed. This will be discussed in Section 3.3.

3.3 Probabilities of Detection and False Alarm

For design and analysis purpose, we formulate the alignment detection as choosing between the following two hypotheses:

$$H_1 \ : \ |e_\tau| \le \tfrac{T_c}{2} \quad or \quad \tfrac{N-1}{2}T_c \le |e_\tau| \le \tfrac{NT_c}{2} \quad \text{(alignment)} \tag{3.33}$$

$$H_0 \ : \ T_c \le |e_\tau| \le \left(\tfrac{N-2}{2}\right)T_c \quad \text{(no alignment).}$$

Therefore, H_1 represents phase alignment case, i.e. the phase error is within $\pm\frac{T_c}{2}$ of the two stable points 0 and $\frac{NT_c}{2}$ in Figure 3.4, while H_0 represent the case that

the phase error is at the least T_c away from the two stable points. Writing the error as $e_\tau = (j+\gamma)T_c$, where j is an integer and $-0.5 < \gamma \le 0.5$, we may write (3.33) as

$$
\begin{aligned}
H_1: \quad & j = 0 \quad \text{and} \quad -0.5 < \gamma \le 0.5 \\
& \text{or } j = -1 \quad \text{and} \quad \gamma = 0.5 \\
& \text{or } j = \tfrac{N-1}{2} \quad \text{and} \quad 0 \le \gamma \le 0.5 \\
& \text{or } j = -\tfrac{N-1}{2} \quad \text{and} \quad -0.5 < \gamma \le 0 \\
H_0: \quad & j \in I = \left\{\tfrac{-N+3}{2}, \tfrac{-N+5}{2}, \ldots, -3, -2, 2, 3, \ldots, \tfrac{N-5}{2}, \tfrac{N-3}{2}\right\} \text{ and } -0.5 < \gamma \le 0.5 \\
& \text{or } j = \tfrac{-N+1}{2} \quad \text{and} \quad \gamma = 0.5 \\
& \text{or } j = -1 \quad \text{and} \quad -0.5 < \gamma \le 0 \\
& \text{or } j = 1 \quad \text{and} \quad 0 \le \gamma \le 0.5.
\end{aligned}
\tag{3.34}
$$

Note that the case when $\frac{T_c}{2} < |e_\tau| < T_c$ and $\left(\frac{N}{2}-1\right)T_c < |e_\tau| < \left(\frac{N-1}{2}\right)T_c$ are not included in either hypothesis, so that there is some distance between H_0 and H_1. Otherwise, the integration length nT_c needs to be excessively large in order that the detector can distinguish between H_0 and H_1, making the acquisition system performance poor.

Detection probability (P_d) and false alarm probability detector (P_{fa}) of the alignment detector are obtained as follows. Detection probability is the probability that phase alignment is correctly detected, which can occur in two situations. First, given that $|e_\tau| < \frac{T_c}{2}$, we obtain detection when the event $A_1 = \{s_1 > s_2\} \cap \{s_1 > \Gamma\}$ is true, where s_1 and s_2 are the test statistics given in Figure 3.1. The second case of detection is obtained when A_2 is true given that $\frac{N-1}{2}T_c \le |e_\tau| \le \frac{N}{2}T_c$, where $A_2 = \{s_2 > s_1\} \cap \{s_2 > \Gamma\}$. The probability of detection is the weighted value of these two values. Letting $B_1 = \left\{|e_\tau| \le \frac{T_c}{2}\right.$ and $B_2 = \left\{\frac{N-1}{2}T_c \le |e_\tau| \le \frac{NT_c}{2}\right.$, we have

$$
P_d = \frac{\Pr(A_1|B_1)\Pr(B_1) + \Pr(A_2|B_2)\Pr(B_2)}{\Pr(B_1) + \Pr(B_2)}. \tag{3.35}
$$

Since e_τ is equally likely to be anywhere in $[0, NT_c]$, we have $\Pr(B_1) = \Pr(B_2) = 1/N$ and

$$
P_d = \frac{\Pr(A_1|B_1) + \Pr(A_2|B_2)}{2}. \tag{3.36}
$$

To compute P_d we note that $s_1 = s_{1,R}^2 + s_{1,I}^2$, $s_2 = s_{2,R}^2 + s_{2,I}^2$ where

$$
s_{1,R} = \sqrt{2P}T_c \cos\theta \int_0^{nT_c} c(t-\hat{\tau}_{ln})c(t-\tau)dt + \int_0^{nT_c} c(t-\hat{\tau}_{ln})z_R(t)dt \tag{3.37}
$$

$$s_{1,I} = \sqrt{2P}T_c \sin\theta \int_0^{nT_c} c(t-\hat{\tau}_{ln})c(t-\tau)dt + \int_0^{nT_c} c(t-\hat{\tau}_{ln})z_I(t)dt \quad (3.38)$$

$$s_{2,R} = \sqrt{2P}T_c \cos\theta \int_0^{nT_c} c(t-\hat{\tau}_{ln}-\tfrac{NT_c}{2})c(t-\tau)dt + \int_0^{nT_c} c(t-\hat{\tau}_{ln}-\tfrac{NT_c}{2})z_R(t)dt \quad (3.39)$$

$$s_{2,I} = \sqrt{2P}T_c \sin\theta \int_0^{nT_c} c(t-\hat{\tau}_{ln}-\tfrac{NT_c}{2})c(t-\tau)dt + \int_0^{nT_c} c(t-\hat{\tau}_{ln}-\tfrac{NT_c}{2})z_I(t)dt. \quad (3.40)$$

Here, $\hat{\tau}_{ln}$ is the phase shift of the local PN signal at time lnT_c. It is shown in Appendix B that

$$P_d = \int_{\Gamma'}^{\infty} \left(1 - Q\left(\sqrt{\tfrac{SNR}{n}}\lambda\left(n,0,\tfrac{N+1}{2}\right), \sqrt{x}\right)\right) f_{s_1'}(x|0,0.5)dx \quad (3.41)$$

where $f_{s_1'}(x|j,\gamma)$ is the pdf of $s_1' \underline{\Delta} s_1 / nN_0T_c$ when $e_\tau = (j+\gamma)T_c$, given in Appendix B, $Q(\cdot,\cdot)$ is the Marcum Q-function defined as

$$Q(a,b) = \int_b^{\infty} xe^{-(x^2+a^2)/2} I_0(ax)dx \quad (3.42)$$

and

$$\lambda(n,\gamma,j) = (1-|\gamma|)\sum_{k=0}^{n-1} c_k c_{k-j} + |\gamma| \sum_{k=0}^{n-1} c_k c_{k-j-\mathrm{sgn}(\gamma)} \quad (3.43)$$

which is described in [25]. Here, $I_0(\cdot)$ is the modified Bessel's function of zeroth order and $\mathrm{sgn}(t) = 1$ if $t \geq 0$ and -1 if $t < 0$.

The false alarm probability is the probability of accepting H_1 given that H_0 is true. When false alarm occurs, the receiver loses some time trying to track the wrong phase. The time spent until the receiver realizes that it cannot track is called penalty time. In this paper a penalty time is assumed to be a multiple of nT_c, i.e.,

$$\text{Penalty time} = K_p nT_c, \quad (3.44)$$

where K_p is some constant. The region of H_0 is in (3.33). Therefore, we define P_{fa} as an average probability given by

$$P_{fa} = \frac{1}{(N-4)T_c} \int_{T_c \leq |e_\tau| \leq \left(\frac{N-2}{2}\right)T_c} P_{fa}(e_\tau)de_\tau \quad (3.45)$$

where

$$P_{fa}(e_\tau) = \Pr\left(\text{accept } H_1 \mid T_c \leq |e_\tau| \leq \left(\tfrac{N-2}{2}\right)T_c\right)$$

$$= 1\text{-Pr}(\, s_1 < \Gamma \text{ and } s_2 < \Gamma | T_c \le |e_\tau| \le (\tfrac{N-2}{2}) T_c)$$

Since $e_\tau = (j+\gamma)T_c$, we write $P_{fa}(e_\tau)$ as

$$P_{fa}(j,\gamma) = 1 - \left[\int_0^{\Gamma'} f_{s_1'}(x|j,\gamma)dx\right]\left[\int_0^{\Gamma'} f_{s_2'}(y|j,\gamma)dy\right]. \tag{3.46}$$

Substitute (3.46) into (3.45) and rewrite the result using Q-function, (3.44) becomes

$$\begin{aligned} P_{fa} = 1 - \tfrac{1}{N-4}\Bigg\{ & \sum_{j\in I}\int_{-0.5}^{0.5}\left[1 - Q\left(\sqrt{\tfrac{SNR}{n}}\lambda(n,\gamma,j),\sqrt{\Gamma'}\right)\right]\left[1 - Q\left(\sqrt{\tfrac{SNR}{n}}\lambda\left(n,\gamma - \tfrac{\text{sgn}(\gamma)}{2}, j + \tfrac{N+\text{sgn}(\gamma)}{2}\right),\sqrt{\Gamma'}\right)\right]d\gamma \\ & + \int_{-0.5}^{0}\left[1 - Q\left(\sqrt{\tfrac{SNR}{n}}\lambda(n,\gamma,-1),\sqrt{\Gamma'}\right)\right]\left[1 - Q\left(\sqrt{\tfrac{SNR}{n}}\lambda(n,\gamma+0.5,\tfrac{N-1}{2}),\sqrt{\Gamma'}\right)\right]d\gamma \\ & + \int_{0}^{0.5}\left[1 - Q\left(\sqrt{\tfrac{SNR}{n}}\lambda(n,\gamma,1),\sqrt{\Gamma'}\right)\right]\left[1 - Q\left(\sqrt{\tfrac{SNR}{n}}\lambda(n,\gamma-0.5,\tfrac{N+3}{2}),\sqrt{\Gamma'}\right)\right]d\gamma\Bigg\} \end{aligned} \tag{3.47}$$

where I is given in (3.34).

Given the desired values of P_d and P_{fa}, the value of n and Γ' can be computed numerically from (3.41) and (3.47).

3.4 Simulation Results

The acquisition time performance of the proposed scheme is evaluated by simulation. We consider both the mean acquisition time and the variance of the acquisition time of the proposed scheme. Moreover, we also compare its performance with the conventional noncoherent serial scheme, which is depicted in Figure 2.2. The PN signal in the simulations is generated from m-sequence with polynomial $h(x) = 1 + x^4 + x^9$, i.e. $N = 511$. A flow chart for simulating of the proposed scheme is presented in Figure 3.6 where the parameter K is the number of trials. Simulations were carried out in 4 cases, with the parameter values shown in Table 3.1. In each case the same SNR, P_d, P_{fa} and K_p were used for both schemes. At the same SNR, P_d, and P_{fa}, the correlation lengths for test alignment of the two schemes are different, as indicated in Table 3.1, because the phase alignment detectors of both schemes are different. These correlation lengths can be computed by numerically solving (3.41) and (3.47) for the proposed scheme and (2.70) and (2.73) of [25] for the conventional scheme. K_p is a parameter independent of SNR, P_d, and P_{fa}. In practice it depends on how long the tracking circuit take of realize a false alarm. To see the effect of K_p, we use two different values of K_p, 20 and 50, while keeping the other parameters the same. In each case of simulation the parameter M of the filter $H(f)$ in the proposed scheme is varied from 500 to 12,000 and K = 2555.

Results of the mean acquisition time and the variance of the acquisition time are given in Table 3.1 for the conventional scheme, while they are plotted in Figures 3.6

Table 3.1:

Parameter values used in the simulation of the proposed noncoherent scheme and performance of the conventional scheme

Case	*SNR* (dB)	P_d	P_{fa}	Correlation time		K_p	Results for Conventional scheme	
				Proposed scheme(n)	Conventional Scheme(n'')		Mean acq. time ($/T_c$)	Variance of acq. time ($/1{,}000T_c$)^2
1	-5	0.9	0.1	179	130	20	90,869	11,825
2	-5	0.9	0.1	179	130	50	147,586	30,130
3	-5	0.95	0.05	240	180	20	85,744	11,271
4	0	0.95	0.05	70	64	20	34,938	1,127

and 3.7 for the proposed scheme. Figures 3.6 and 3.7 show that the mean and variance are reasonably stable for a wide range of M. When M is too small, the acquisition time of the proposed scheme increases. Recall that MT_c is the length of the filter in the VCC loop. Therefore, a small M will make the filter less effective in filtering out noise. On the other hand, if M too large, the VCC loop will take unnecessarily long time to perform the filtering, leading to inefficiency.

To compare the two schemes, we define two ratios R_1 and R_2 as

$$R_1 = \frac{\overline{T}_{\text{non,serial}}}{\overline{T}_{\text{non,close}}} \tag{3.48}$$

where $\overline{T}_{\text{non,serial}}$ is the mean acquisition time of the conventional scheme and $\overline{T}_{\text{non,close}}$ is the mean acquisition time of the proposed scheme, and

$$R_2 = \frac{\sigma^2_{\text{non,serial}}}{\sigma^2_{\text{non,close}}} \tag{3.49}$$

where $\sigma^2_{\text{non,serial}}$ is the variance of the acquisition time of the conventional scheme and $\sigma^2_{\text{non,close}}$ is the variance of the acquisition time of the proposed scheme. Results for R_1 and R_2 are plotted in Figures 3.8 and 3.9, respectively. From Figure 3.8, we see that the proposed scheme acquires the correct phase three to four times faster than the conventional scheme. In Figure 3.9 we see that the variance of the acquisition time of the proposed scheme is smaller than that of the conventional scheme by 20 to 40 times.

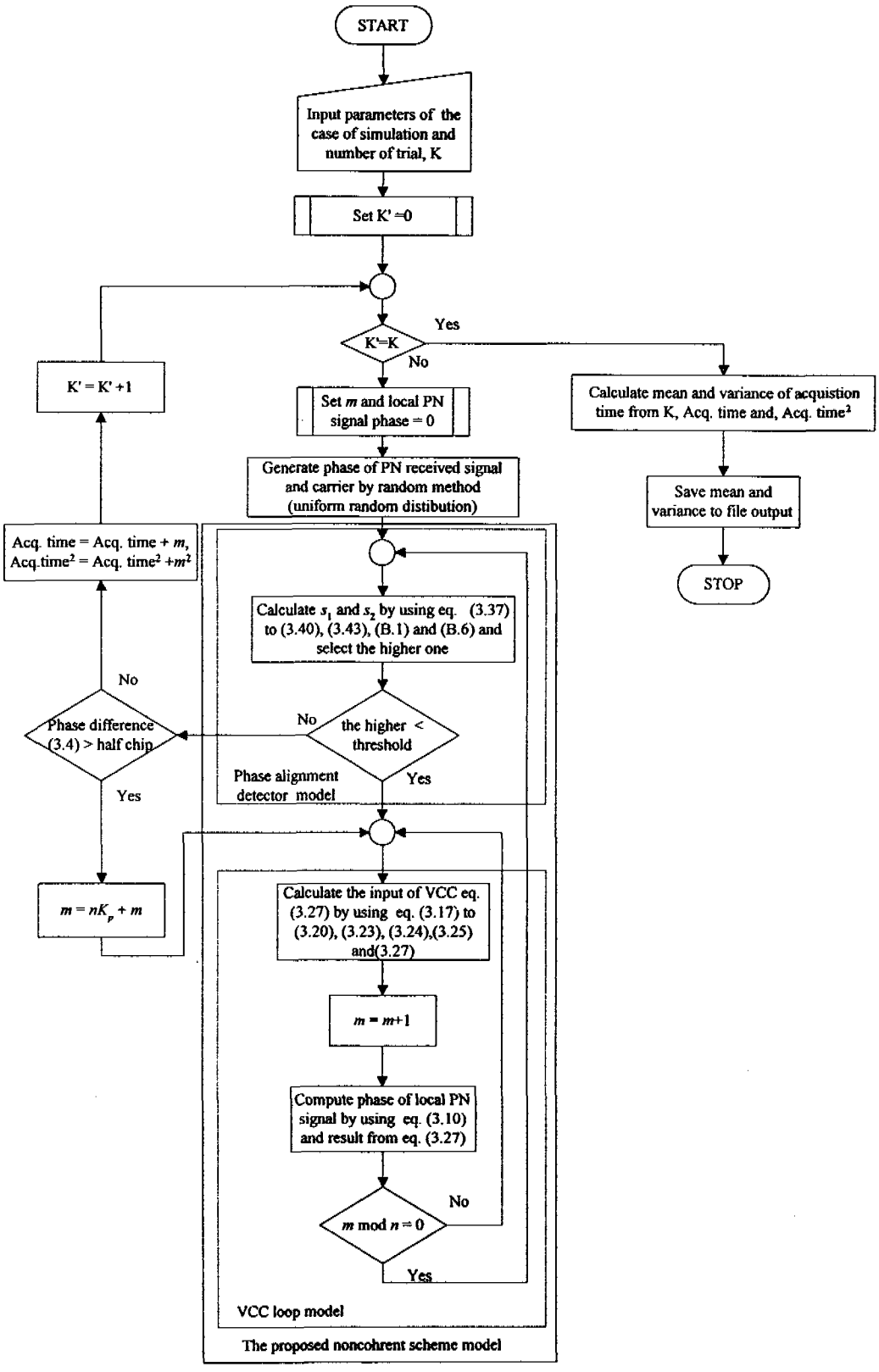

Figure 3.5: Flowchart of the simulation program for the proposed noncoherent scheme

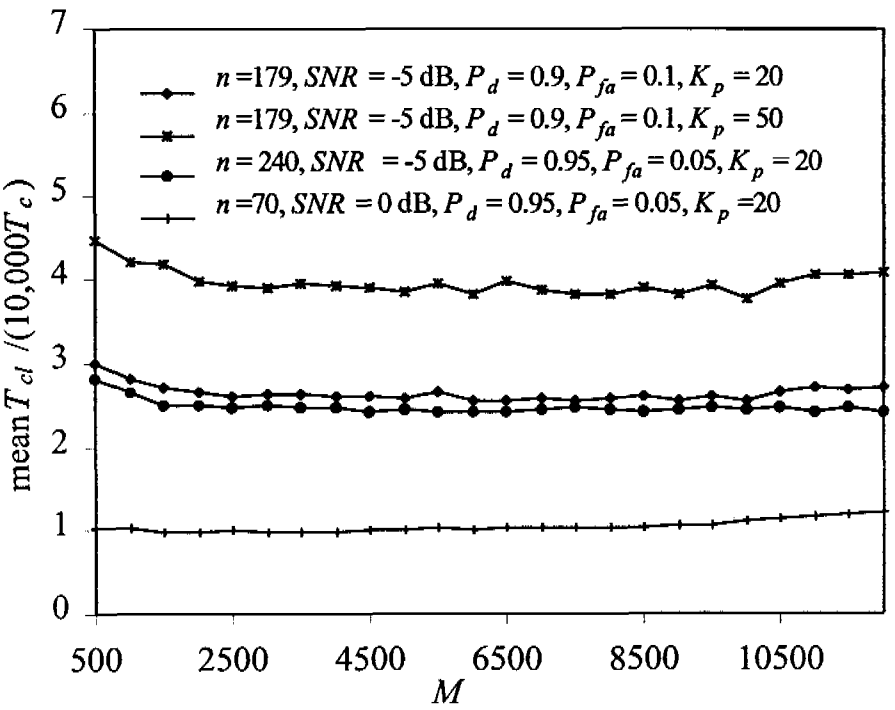

Figure 3.6: Mean acquisition time of the proposed scheme

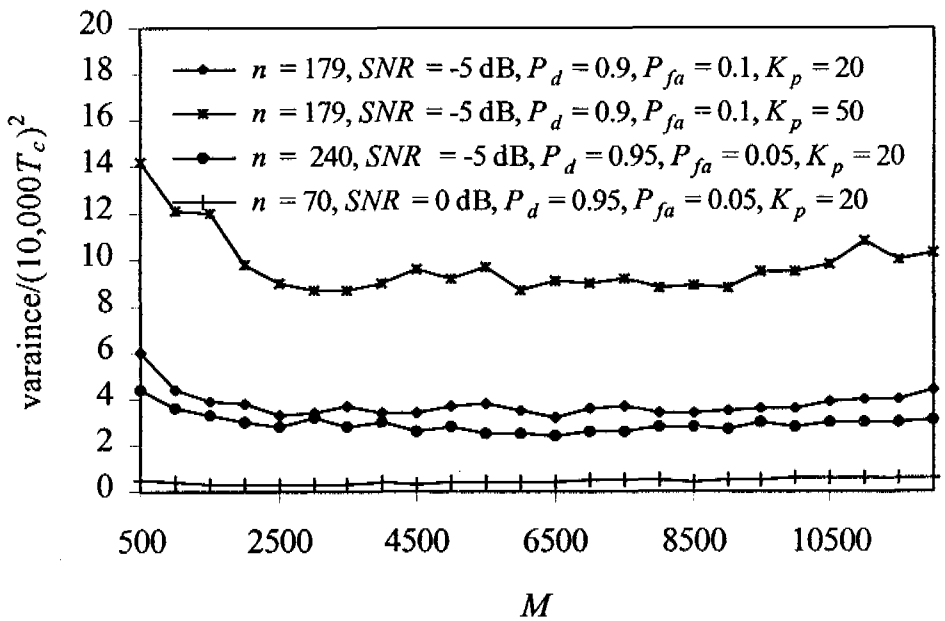

Figure 3.7: Variance of the acquisition time of the proposed noncoherent scheme

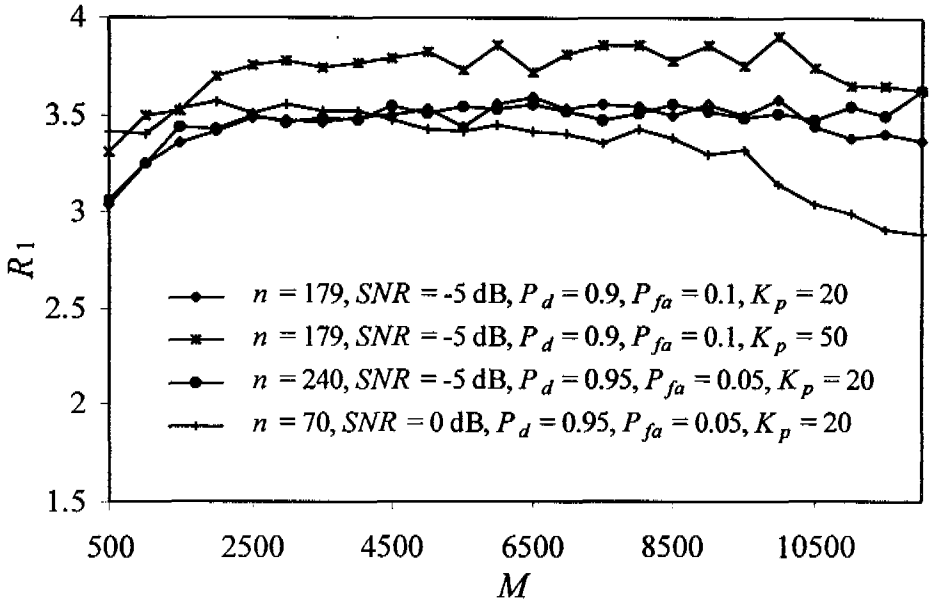

Figure 3.8: Ratio of the mean acquisition time of the conventional noncoherent serial scheme to that of the proposed scheme

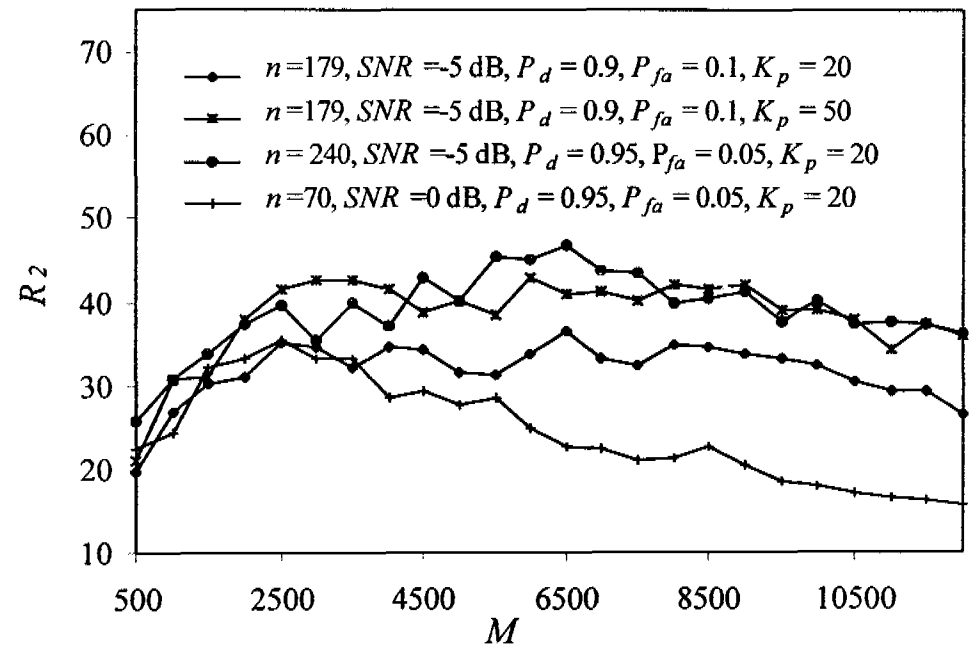

Figure 3.9: Ratio of the variance of the acquisition time of the conventional noncoherent serial scheme to that of the proposed scheme